

Article

Analysis of Influencing Factors in Pilot Experiment for Synthesis of Natural Gas Hydrate by Spray Method

Yun Ma ¹, Jinzhao Zhu ², Qingguo Meng ^{3,4,*} , Chunxiao Ding ^{2,5}, Jinbing Teng ², Xin Wang ¹ and Qian Lu ¹¹ School of Civil Engineering, Yangtze Normal University, Chongqing 408100, China² Linyi Special Equipment Inspection Institute, Linyi 276002, China³ The Key Laboratory of Natural Gas Hydrate, Ministry of Natural Resources, Qingdao Institute of Marine Geology, Qingdao 266237, China⁴ Laboratory for Marine Mineral Resources, Laoshan Laboratory, Qingdao 266237, China⁵ School of Marine Earth Sciences, Ocean University of China, Qingdao 266100, China

* Correspondence: mengqing@126.com

Abstract: In recent years, the technology of storing and transporting natural gas in the form of hydrate has received a lot of attention. At present, the research on the synthesis of natural gas hydrate for the purpose of storage and transportation is still in the laboratory stage, and its synthesis process is in the design and conception stage. The influencing factors of natural gas hydrate synthesis under pilot-scale conditions are more complex. Moreover, pilot experiments are oriented to actual production, and its economic feasibility and operational convenience have higher requirements. This paper aimed to study the influencing factors of gas hydrate synthesis by spray method under pilot-scale conditions. Under specific conditions of surfactant and pressure, we carried out research on the effects of reaction temperature, different forms of atomizers, high-pressure pump flow, experimental water, and other factors. Experiments show that the optimal synthesis conditions were a temperature of $-5\text{ }^{\circ}\text{C}$, a pressure of 5 MPa, a conical nozzle, a generated gas hydrate as the hydrate of type I structure, and a gas storage capacity of 1:123 (gas–water ratio).

Keywords: natural gas hydrate; artificial synthesis; pilot-scale experiment; spray method



Citation: Ma, Y.; Zhu, J.; Meng, Q.; Ding, C.; Teng, J.; Wang, X.; Lu, Q. Analysis of Influencing Factors in Pilot Experiment for Synthesis of Natural Gas Hydrate by Spray Method. *Processes* **2022**, *10*, 2740. <https://doi.org/10.3390/pr10122740>

Academic Editors: Tao Yu, Zhenyuan Yin, Bingbing Chen, Pengfei Wang and Ying Teng

Received: 11 November 2022

Accepted: 13 December 2022

Published: 19 December 2022

Publisher's Note: MDPI stays neutral with regard to jurisdictional claims in published maps and institutional affiliations.



Copyright: © 2022 by the authors. Licensee MDPI, Basel, Switzerland. This article is an open access article distributed under the terms and conditions of the Creative Commons Attribution (CC BY) license (<https://creativecommons.org/licenses/by/4.0/>).

1. Introduction

Natural gas hydrate is a clathrate crystalline compound formed by one or more hydrocarbon gases reacting with water at a certain temperature and pressure [1]. It is globally recognized as a new type of clean energy due to its large global reserves, wide distribution, and clean combustion. With the deepening of research, more and more scholars have found that conventional natural gas can be prepared into solid hydrate for storage and transportation. It is believed that the natural gas hydrate storage and transportation technology may replace the liquefied natural gas technology and become one of the large-scale natural gas storage and transportation methods in the future [2–6].

Since Dr. Gudmundsson et al. advocated the idea of ocean transportation of natural gas by means of natural gas hydrate (NGH) in 1996 [7], technical research on hydrate formation storage and transportation has been carried out abroad and gradually used for commercial development [8–14], such as in the case of the Marathon Oil Corporation in the United States and in certain cases in Southeast Asia with the Mitsui Engineering and Shipbuilding Co.(MES) in cooperation with six Japanese leading companies related to natural gas businesses.

However, hydrate storage and transportation technology is still in the laboratory development stage in China, and has not yet formed a large-scale commercial application [15–18]. The economical and efficient synthesis of solid hydrates is the key to the industrialization of this technology. In terms of the synthesis of hydrates, scholars at home and abroad have completed many useful explorations. Scholars have focused on two

aspects of hydrate formation conditions and synthesis rates, mainly through three types of methods: strengthening test equipment, strengthening physical conditions (nanofluid, external field action), and strengthening chemical reagents to improve hydrate phase equilibrium conditions, increase gas–liquid contact area, enhance heat transfer efficiency, and improve gas solubility [19–28]. Rogers et al. first used an ultrasonic sprayer to spray water into a low-temperature pressurized reactor, reducing the diameter of the water mist droplets to about 90 μm , which enlarged the contact area between water and gas by about 60 times [29]. Xie et al. found that the hydrate synthesis efficiency was higher in continuous intakes than in intermittent intakes through experiments [30]. Zhou et al. believed that the high airflow rate and prolonged ventilation time could shorten the induction period of hydrate synthesis by about two thirds [31]. Hu et al. pointed out that the selection of nozzles was very important in the experiment of preparing hydrate by spraying and believed that a suitable nozzle could not only increase the contact area of gas and water, but also strengthen heat and mass transfer [32]. Yang et al. used the spray method to improve the binding rate of water molecules and gas molecular groups and expand the contact area to enhance the rate of hydrate formation [33]. Liu et al. inted out that spraying measures could effectively shorten the induction time of hydrate formation. When the initial water temperature was constant, the higher the initial pressure of the system, the shorter the induction time; when the initial pressure was constant, the lower the initial water temperature was, the shorter the induction time was [34]. Zhang et al. proposed a spray-enhanced continuous hydrate preparation device, which used an induction reactor and a main reactor to separate and control the induction reaction and the rapid crystallization reaction, which facilitated the efficient preparation of hydrates [35]. Hu et al. also pointed out that adding an appropriate concentration of SDS (sodium dodecyl sulfate water solution) in the spray system could raise the average hydrate formation rate 1.5 times, while enhancing the gas storage capacity of hydrate [36]. Song believed that under the conditions of temperature (275.15 K), pressure (5.0 MPa), and 500 r/min stirring driving conditions, the SH-type natural gas hydrate could be rapidly synthesized by using methylcyclohexane and methyl tert-butyl ether with the addition of 0.25% surfactant SDS or rhamnolipid [37]. Shi [38] and Lin et al. [39] studied the effect of amino acids and nanosphere promoters on hydrate synthesis and proposed that amino acids could reduce hydrate growth conditions and enhance later growth, and spiral stirring could ensure the excellent hydrate formation in the early reaction. Zhong et al. found that the critical micellar concentration (CMC) of sodium dodecyl sulfate water solution was 242 ppm at hydrate forming conditions, and above this value, the hydrate synthesis speed increased at a high speed [40].

To summarize, the synthesis of natural gas hydrate in the current hydrate storage and transportation method is still in the experimental stage, and there are very few pilot-scale experimental studies. The commercial application of this technology is not yet imminent. Based on previous research results, the SDS-based spray method to synthesize hydrate is the preferred way to promote the industrialization of gas hydrate synthesis technology. In this experiment, the experiment of artificial synthesis of natural gas hydrate by spray method in pilot scale was further analyzed, and the feasibility of the synthesis method was verified. Under the conditions of surfactant SDS and certain pressures, we studied the effects of reaction temperature, different forms of atomizers, high-pressure pump flows, experimental water, and other factors. This provides a reference for the industrialization of hydrate storage and transportation methods at a later stage.

2. Materials and Methods

2.1. Experimental Setup

As shown in Figures 1 and 2, the inner volume of the reactor was 0.248 m^3 , the design pressure was 13.20 MPa, and the design temperature was $-20\sim 50$ $^{\circ}\text{C}$. The heat exchange area of the heat exchange tube in the reaction kettle was 1.47 m^2 and the volume was 0.003 m^3 . The opening of the heat exchange tube was connected to the refrigerant at the bottom of the lower head of the reaction kettle. The outer body of the reaction kettle

was covered with a thermal insulation layer. The pressure gauge and thermometer were installed in the middle of the side wall of the reactor. The spray inlet was about 40 mm from the edge of the top of the head on the reactor.



Figure 1. Reactor equipment.

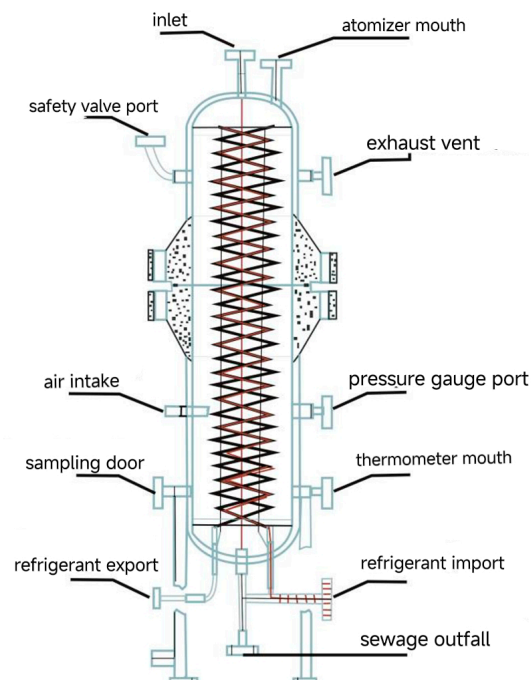


Figure 2. Schematic diagram of main structure of the reactor.

In order to verify and efficiently prepare hydrate during the experiment, four kinds of atomizers were used as a comparison, and the parameters are shown in Table 1.

Table 1. Parameter table of different atomizers.

Atomizer Types	Orifice Diameter (mm)	Flow Rate Under 0~0.2 MPa Pressure (L/h)	Jet Angle (°)	Temperature Reflex (°C)
Fine Atomizing Rotary Vane Atomizer	0.7	0~12	40	4
Stainless-steel Atomizer 1	0.79	0~35	52~58	-5
Stainless-steel Atomizer 2	2	0~100	77~82	-5
Conical Atomizer	1.5	0~114	52~65	-5

The circulating refrigeration temperature control system was a MLZ021 unit, and the refrigerant was R404A.

Two kinds of high-pressure pumps were used in this test and the parameters were in the Table 2:

Table 2. The parameter tables of the two kinds of high-pressure pumps.

Pump Types	Flow (L/h)	Greatest Pressure (MPa)
Advection pump	1.8	40
Reciprocating Piston Pump	22	60

An inVia Laser Raman Spectrometer (Renishaw, London, UK) was used from the Qingdao Institute of Marine Geology which was equipped with a low temperature cold table to ensure that there was no decomposition during the sample experimenting process. The excitation wavelength was Ar⁺ laser 514.5 nm and the power was 20 mW. This spectrometer was equipped with a Leica high-performance microscope, whose confocal effect could achieve a spatial resolution of less than 1 μm laterally and about 2 μm in depth. The number of grating lines was 2400 lines/mm. The laser entered the microscope through a high-efficiency optical fiber, and a 20× objective lens was used [4].

The gas storage capacity measurement device had a vacuum degree of the vacuum pump of ≤ -95.0 KPa [41], as shown in Figure 3. The pressure sensor display range was -100 to 300 KPa and the temperature accuracy was ±0.1 °C.

**Figure 3.** Gas storage capacity measurement device.

2.2. Experimental Reagents and Materials

Four kinds of reagents and materials were used in this test, they were showed in the Table 3:

Table 3. Experiment Reagents and Materials List.

Reagents and Materials	Element
Natural gas	CH ₄ 93.255%, C ₂ H ₆ 3.2028%, C ₃ H ₈ 0.6897%, Other alkane gases 0.8955%, N ₂ 0.8236%, CO ₂ 1.1334%
Surfactant	C ₁₂ H ₂₅ SO ₄ Na (SDS)
Deionized water	H ₂ O
Tap water	H ₂ O with some impurities

3. Synthesis Process and Experimental Observation Results

3.1. Synthesis Process

- (1) First, we turned on the circulating refrigeration temperature control system, and set the temperature to the initial reaction temperature (see Table 4 for the initial temperatures under various working conditions).

Table 4. Experimental conditions and parameters.

Working Conditions	Condition 1	Condition 2	Condition 3	Condition 4	Condition 5	Condition 6		
Types of Pump	Advection Pump	Piston Pump	Piston Pump	Piston Pump	Piston Pump	Piston Pump		
Solution category	Deionized water	Deionized water	0.35 g/L SDS Deionized water solution	0.35 g/L SDS Deionized water solution	0.35 g/L SDS Deionized water solution	0.5 g/L SDS Tap water solution		
Initial pressure (MPa)	6	6	5	5	5	5		
The initial temperature (°C)	2	2	4	0	−5	−5		
Ambient temperature (°C)	−6–1	−1–11	3–9	16–19	18–20	18–20		
Water intake time (H)	28	2	2	2	2	2		
Water intake (L)	50.4	40	40	40	40	40		
Test times	3	2 times per nebulizer	3	3	3	3		
Sample detection method	Raman spectroscopy	Raman spectroscopy	Raman spectroscopy	Raman spectroscopy	Raman spectroscopy	Raman spectroscopy		
Atomizer	Conical	Conical Atomizer	Stainless-steel Atomizer 1 Stainless-steel Atomizer 2	Fine Atomizing Rotary Vane Conical Atomizer	Stainless-steel Atomizer 1 Stainless-steel Atomizer 2 Conical Atomizer	Conical Atomizer		
Hydrate formation and combustion	No	No	Yes, small flame and short burning time	Yes, small flame and burns instantaneously	Little, no flame	Yes, small flame and short burning time	Yes, big flame and lasts a long time	Yes (type I structure) big flame and lasts a long time
State	Whole ice cubes	Colorless or pale yellow, translucent ice cubes and ice residues	Soft ice-like solid	Snow-like, slightly watery	Loose snow	Soft ice-like solid	Hard solid ice	Hard solid ice
Distribution	At the bottom of the reactor	At the bottom of the reactor	Inside the atomizer, the water spray gap and around the atomizer, blocking the atomizer	Permeates the entire space in the reactor	At the bottom of the reactor	Extends from one side of the atomizer to the other side of the barrel	From the cylinder wall on one side of the atomizer to the spray range and the bottom of the head of the reactor	From the cylinder wall on one side of the atomizer to the spray range and the bottom of the head of the reactor

- (2) After the pressure was reduced to 6–7 MPa by the pressure reducer of the cylinder group, the natural gas was slowly filled into the reaction kettle until the pressure

reached the initial reaction pressure (see Table 4 for the initial pressure under various working conditions).

- (3) During the process of slowly filling the reaction kettle with natural gas, the discharge valve was opened slightly. On the one hand, it replaced the air in the reactor, and on the other hand, it helped to increase the pressure of the reactor. It was slowly filled for about 1 min then the discharge valve was closed. The air in the reactor was exhausted at this time.
- (4) The change of the pressure gauge of the reaction kettle was observed. When the pressure of the pressure gauge reached the initial pressure required for the experiment, we stopped feeding the natural gas. After 30 min of stabilization, we adjusted the intake air so that the pressure value indicated by the pointer of the pressure gauge was the pressure required for the experiment.
- (5) The high pressure pump was turned on, the solution (deionized water, or SDS deionized water solution or SDS tap water solution) pumped into the atomizer (a valve was installed at the inlet end of the atomizer) and then entered the reactor.
- (6) The thermometer of the reaction kettle was observed constantly and the circulating refrigeration temperature control system was kept running automatically.
- (7) In the process of entering the solution, the changes of temperature and pressure in the reactor were observed carefully.
- (8) The temperature of the reaction kettle was kept at the temperature of step (1), after the completion of water feeding, it was left to stand for 1 h. When the pressure in the reactor did not change within 30 min, the reaction was terminated.

We observed, recorded, and measured the results, and each group of experiments was repeated three times.

3.2. Product Detection Method—Raman Spectrometry

The samples were placed in a cold stage at $-190\text{ }^{\circ}\text{C}$. The laser excitation wavelength was 514.5 nm , the exposure time was 10 s , the scanning range was $100\text{--}4000\text{ cm}^{-1}$, the slit width was $65\text{ }\mu\text{m}$, and the $20\times$ telephoto objective was used. Taking the sample detection of working condition 6 as an example, the Raman spectrum of the synthesized natural gas hydrate after measurement is shown in Figure 4.

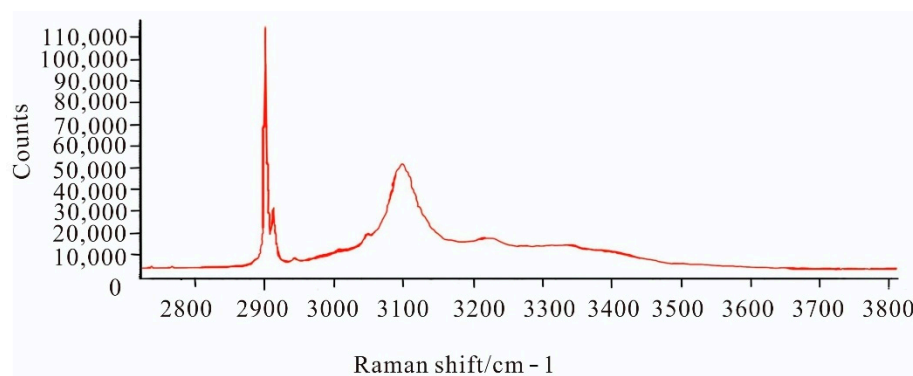


Figure 4. Laser Raman spectrum of gas hydrate.

The stretching vibration peaks of C-H bond (methane) and O-H bond (bound water) in the sample were around 2910 cm^{-1} and 3105 cm^{-1} , respectively. The C-H bond split two peaks at 2901 cm^{-1} and 2912 cm^{-1} . Compared with the C-H bond Raman spectrum peak of pure methane gas at 2916 cm^{-1} [42], both peaks of the hydrate sample were shifted to the left, mainly due to the perturbation of the electrostatic field of the water molecules forming the cages. The Raman peak of methane split around 2916 cm^{-1} due to the different spatial structures of the large cage and the small cage and the attraction to methane molecules being slightly different. The peak at 2901 cm^{-1} represents the frequency of methane molecules in the large cage, 2912 cm^{-1} represents the frequency of methane molecules in the small cage.

Among them, the Raman intensity (peak area) ratio of the large cage and the small cage was basically 3:1, which is in line with the theoretical spatial structure that each unit cell of the I-type structure hydrate crystal consists of 6 large cages and 2 small cages.

The spectral peak near 3105 cm^{-1} should be the stretching vibration peak of the O-H bond, which is the vibration peak of water in hydrate. In the interaction between the methane molecule and the water molecule, the spectral peak of the water molecule also shifted. Meng et al. measured the Raman peak position of water in SDS-methane hydrate at around 3088 cm^{-1} , which is slightly different from our experimental results [43].

3.3. Test Methods for Gas Storage

The gas storage capacity testing device was self-designed, and the design principle was based on the patent of Ye et al. [41]. The vacuum volume method was used to measure the gas storage capacity of hydrates. Taking the sample of working condition 6 as an example, the gas storage capacity of the obtained synthetic natural gas hydrate was 1:123 (gas–water ratio).

The volume of standard tube A was $V_0 = 30\text{ mL}$. The pressure after vacuuming before the test was $P_a = -95.3\text{ kPa}$. Valve 1 and valve 2 were closed, and the pressure after opening valve 3 was $P_b = -13.5\text{ kPa}$. The standard pipe gas pressure was $P_0 = P_a - P_b = -95.3\text{ kPa} - (-13.5\text{ kPa}) = -81.8\text{ kPa}$. The liquid nitrogen was removed and the pressure value after the temperature rose to room temperature was $P_c = 8.7\text{ kPa}$. The gas pressure in standard pipe A was $P_1 = P_a - P_c = -95.3\text{ kPa} - 8.7\text{ kPa} = -104\text{ kPa}$. The volume of natural gas released after hydrate decomposition was $V_1 = (-104) \times 30 / (-81.8) = 38.14\text{ mL}$. The weight of sample tube B (sample tube + water remaining after hydrate decomposition) was $W_1 = 38.9599\text{ g}$. The weight of the sample tube B after the moisture in the sample tube was dried was $W_2 = 38.6503\text{ g}$. So we got the weight $W_{\text{H}_2\text{O}} = W_1 - W_2 = 0.3096\text{ g}$. The density of water at $20\text{ }^\circ\text{C}$ was $\rho_{\text{H}_2\text{O}} = 0.998\text{ g/cm}^3$. The volume of decomposed water in the hydrate was $V_{\text{H}_2\text{O}} = W_{\text{H}_2\text{O}} / \rho_{\text{H}_2\text{O}} = 0.3102\text{ mL}$. Finally, we calculated that $S = 38.14\text{ mL} / 0.3102\text{ mL} \approx 123$.

3.4. Working Conditions and Experimental Observations

We repeated the experimental steps of 2.1 with different pumps, different solutions, and different sprayers. The experimental conditions were set and the observed results are shown in Table 4.

Condition 1: The basic situation of this condition is shown in Table 4. It should be emphasized that the flow rate of the advection pump was too small, and the water sprayed through the atomizer could not achieve the atomization effect, and only entered the reaction kettle in the form of water droplets. After the experiment was completed, there were integral ice cubes in the kettle and no effective hydrate was detected.

Condition 2: In view of the situation of the working condition 1, the plunger pump with large flow replaced the previous one and matched the conical atomizer, stainless-steel atomizer 1, and stainless-steel atomizer 2. Other conditions remained unchanged, and each atomizer was tested twice. The samples obtained in the experiment were all colorless or pale yellow, translucent ice cubes, and ice slag. No valid gas hydrates were detected in the samples.

Condition 1 and Condition 2 showed that increasing the flow rate of the pump and matching with the atomizer could achieve a good atomization effect. But no active agent was added in both working conditions which test reagent were both the atomized deionized water and the methane. The direct synthesis of atomized deionized water and methane gas had a very slow or almost no reaction, and the effect was very poor. Therefore, in the latter cases of 3, 4, 5, and 6, the pump was improved and the surface active agent (SDS) was added. Continuing the experiment, we found that:

Condition 3: We added surfactant (SDS) and chose four different atomizers. After the experiment, hydrates were formed in the reaction kettles, which shows that the surfactant plays an important role in the laboratory synthesis of hydrates. Table 5 lists the parameters

of the four types of atomizers. These parameters combined with Table 4, demonstrate that the smaller the atomization particle size, the more sufficient the contact with the gas, and the shorter the time to generate hydrate. However, when the hydrate is produced industrially, the atomized particle size should be carefully selected to prevent the hydrate form too fast to block the nozzle. Of the four nebulizer types tested, the conical nebulizer was the most suitable for the more sustained and efficient synthesis of solid hydrates.

Table 5. Comparison of atomizer parameters and experiment results.

Working conditions		Condition 3		
Types of pumps		Piston Pump		
Solution category		0.35 g/L SDS deionized water solution		
Initial pressure (Mpa)		5		
Initial temperature (°C)		4		
Atomizer types	Fine atomizing rotary vane high pressure atomizer	Conical Atomizer	Stainless-steel Atomizer 1	Stainless-steel Atomizer 2
Nebulizer pressure conditions (Mpa)	0–0.5	0–0.2	0–0.2	0–0.5
Atomizer orifice diameter (mm)	0.7	1.5	0.79	2
The maximum open diameter of the atomizer (mm)	0.5	1.0	0.64	1
Atomizer jet angle (°)	40	52–65	52–58	77–84
Atomizer flow (L/H)	0–20	0–114	0–35	0–150
Experimental results	Hydrate formation time	Instant generation, extremely fast	Fast	Slowly
	Hydrate state	Hard	Hard	Loose snowflake
	Whether hydrate is formed inside the atomizer	Yes	No	No
	Does the atomizer nozzle generate hydrates	Yes	No	No
	Is there a blockage	Yes	No	No
	Gas storage	1:145	1:35	Low

The difference between the experimental conditions of working condition 4 and working condition 5 was in the setting of the initial temperature of the reaction. After the experiment, it was found that the hydrate solid generated by the initial reaction temperature of $-5\text{ }^{\circ}\text{C}$ in working condition 5 was harder and the gas storage capacity was higher. This temperature was more suitable than the initial reaction temperature of $0\text{ }^{\circ}\text{C}$ in Case 4.

The difference between the experimental conditions of condition 5 and condition 6 was in the reaction solution. Condition 5 had SDS deionized water solution and condition 6 had SDS tap water solution. The temperature was set at the optimal reaction temperature $-5\text{ }^{\circ}\text{C}$ which was verified by this experiment. After the experiment, solid hydrates were well synthesized, and the gas storage capacity was not much different. The gas storage capacity of condition 5 was 1:121, and the gas storage capacity of condition 6 was 1:123.

Figure 5 shows curves of temperature and pressure change with time in the reactor on condition 1 to condition 6.

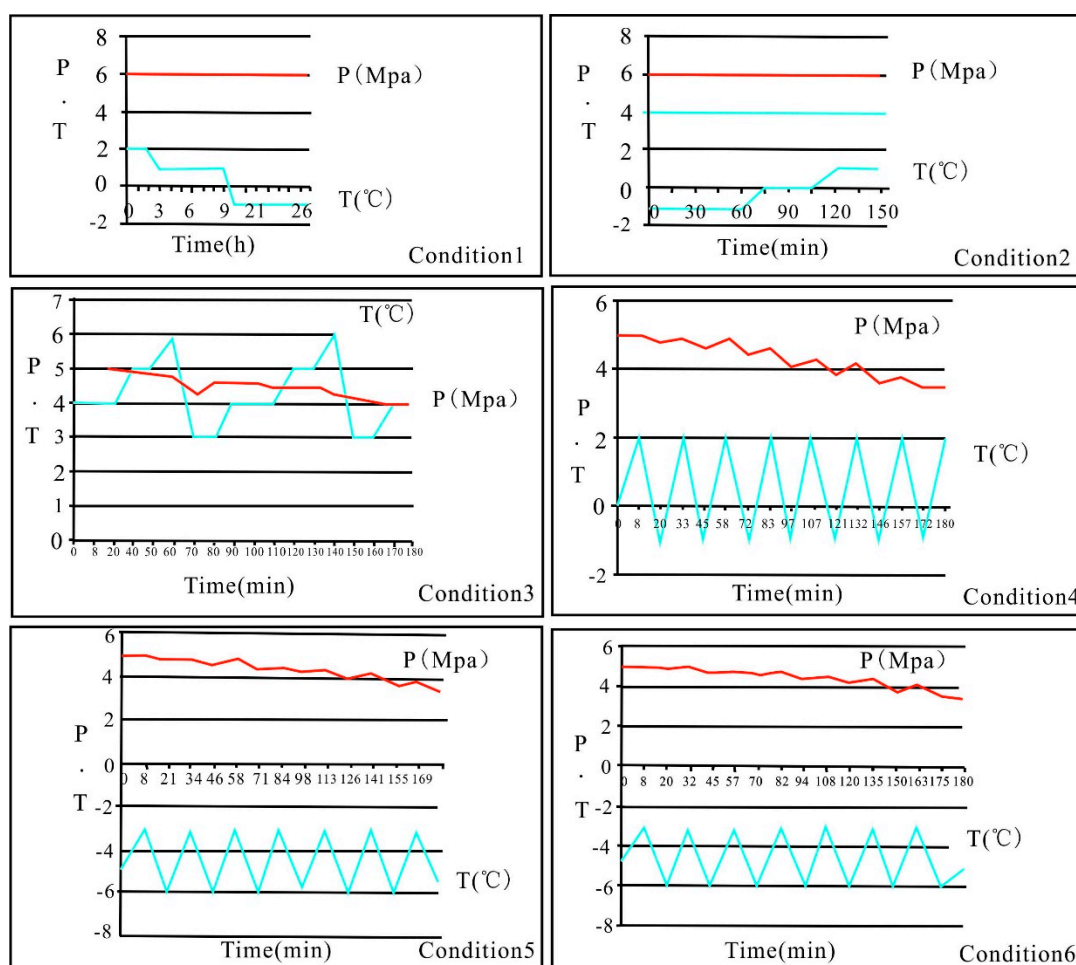


Figure 5. Curves of temperature and pressure change with time in the reactor.

Condition 1: The pressure was constant at 6 Mpa. Because the ambient temperature was reduced, the temperature in the kettle decreased from 2 °C to 1 °C and decreased to below 0 °C at 9 h. Ice began to form in the kettle, and the temperature was further reduced to −1 °C until the end of the experiment.

Condition 2: The pressure was still constant at 6 Mpa. Since the ambient temperature was lower than −1 °C, the temperature control system of circulating refrigeration did not start, so even though the initial reaction temperature was set at 2 °C, the actual reaction temperature was still not −1 °C. However, the ambient temperature increased later. The temperature in the kettle increased from −1 °C to 0 °C one hour after the experiment started, and increased to 1 °C at 105 min.

Condition 3: The temperature in kettle fluctuated within the range of 4 °C–6 °C. Since the ambient temperature was higher than the temperature in the kettle, the circulating refrigeration system was opened to ensure the set temperature. However, the intermittent opening of the circulating refrigeration system caused a certain fluctuation of the natural gas pressure in the reactor.

Condition 4: The frequency of temperature change was higher than that of condition 3 because the starting time interval of the circulating refrigeration system was shortened, and the pressure drop was slightly greater than that of condition 3. On the one hand, the temperature difference between the inside and outside of the reactor became larger due to the increase of the external ambient temperature. On the other hand, it also showed that the heat generated in the reaction process was higher than that in condition 3.

Conditions 5 and 6: The reaction temperature fluctuated within the range of $-6\text{ }^{\circ}\text{C}$ – $-3\text{ }^{\circ}\text{C}$, and the pressure tended to decrease gradually and fluctuated with the change of temperature during the reaction process and the standing process.

Figure 6 shows the synthetic products and their distribution and state in the reactor curves of temperature and pressure changes with time in the reactor under condition 1 to condition 6.



Figure 6. The synthetic products and their distribution and state in the reactor.

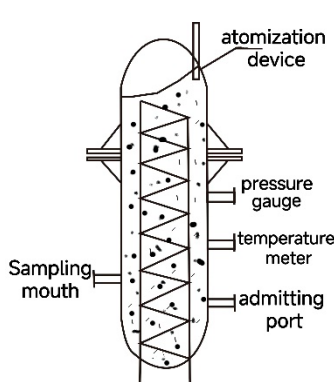
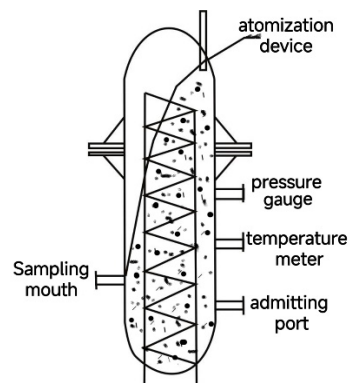
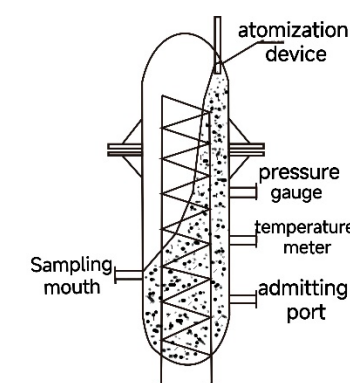
4. Results and Discussion

The results from previous research and the results of this experiment both show that when the pressure is 5 Mpa, it is the ideal pressure for synthesizing hydrates. The discussion of other influencing factors in this paper was set under this pressure to ensure that the relevant unified laws were revealed to their greatest extent. When the temperature of the thermometer was $4\text{ }^{\circ}\text{C}$, $0\text{ }^{\circ}\text{C}$, and $-5\text{ }^{\circ}\text{C}$, we carefully observed and analyzed the experimental results. When the reaction was completed, we released the pressure. We observed the pointer of the pressure gauge to see if it would return to zero. If it returned to zero, it meant that there was no internal gas to continue to discharge, and the hydrate was either not decomposed or the decomposition was completed. If the pressure gauge could not return to zero in time, the pointer vibrated near zero which indicated that not only the remaining natural gas in the inner space of the reactor was being discharged, but also that the natural gas was released by natural gas hydrate. We then closed the valve to stop the exhaust and observed the pressure gauge. If the pressure gauge started to increase slowly, it meant that the natural gas in the hydrate was still being released. When the pointer of the pressure gauge was near a certain pressure, the pressure no longer rose significantly which indicated that the decomposition of hydrate had stopped.

4.1. Influence of Temperature on the Formation, Decomposition, Distribution, and Gas Storage of Hydrate

When the pressure was 5 Mpa, the field tests of working conditions 3, 4, and 5 with the same atomizer, plunger pump, and solution were compared. Table 6 shows the reaction results under different temperature conditions.

Table 6. Comparison for field observation.

Working Condition		Condition 3	Condition 4	Condition 5
Initial Temperature (°C)		4	0	−5
Hydrate state		Snow-like, slightly watery	Soft ice-like solid	Relatively hard solid ice
Burning state		Instant flame	Small flames, short duration	Big flames, long lasting
Decompression	Initial pressure relief	Pressure is around 0 Mpa, the pointer does not swing back to zero and the hydrate is still released	Pressure is around 3.3 Mpa. Slight cracking sound, the hydrate begins to decompose	Pressure is around 3 Mpa. Clear cracking sound, the hydrate begins to decompose
	Close the valve	Pressure rises and hydrate continues to decompose	Stable pressure	Stable pressure
	Stable pressure	Pressure = 1.0 Mpa	Pressure = 0 Mpa	Pressure = 0 Mpa
	Open the lid	A large amount of gas is ejected	A moderate amount of gas is ejected	A small amount of gas is ejected
Hydrate distribution				
	Permeates the entire space in the reactor	Mainly extends from one side of the atomizer to the other side, and the heat exchange tube on the sampling port side is not covered by any hydrate	Distributed from the cylinder wall on one side of the atomizer to the spray range of the atomizer and the bottom of the head of the reactor	
	gas storage	1:35	1:80	1:121

The observation results show that when the pressure is constant, temperature is one of the most important factors affecting the synthesis state, distribution, gas storage, and decomposition of hydrate.

- (1) The compactness of the synthesized hydrate was affected: the higher the reaction temperature, the looser the generated hydrate; the lower the temperature, the denser and harder.
- (2) The gas storage capacity was affected: In this experiment, the lower the reaction temperature, the higher the gas storage capacity of the hydrate sample; conversely, the higher the reaction temperature, the lower the gas storage capacity of the hydrate sample.
- (3) The distribution of synthesized hydrates was affected: the lower the reaction temperature, the more concentrated the distribution of natural gas hydrates in the reactor; the higher the reaction temperature, the more diffuse the hydrates in the reactor space.
- (4) The decomposition of the synthesized hydrate was affected: the lower the temperature, the less natural gas escaped from the hydrate during the exhaust pressure relief process; the higher the temperature, the more natural gas escaped.

4.2. Influence of Water Spray Flow and Atomization Effect of Atomizer on Gas Storage Capacity of Hydrate

In this experiment, four atomizers were selected to repeat the hydrate synthesis experiment. Table 6 shows the types and main parameters of the atomizer and also shows the experimental results under working condition 3.

We found that in the case of a certain pump or the pump body of this experiment:

- (1) The smaller the nozzle hole diameter of the atomizer, the smaller the atomized particles, the better the atomization effect, and the faster the hydrate generation speed. However, the fine atomizing rotary vane high-pressure atomizer formed hydrate almost at the moment of spraying water, and also rapidly formed hydrate inside the atomizer, the gap where the atomizer sprays water outward, and around the atomizer. This blocked the atomizer and caused the reaction to terminate, so the atomization aperture should be suitable for continuous industrial production.
- (2) The pore size of the atomizer nozzle affected the gas storage capacity of the generated hydrate. The smaller the pore size, the harder the hydrate formation texture and the higher the gas storage capacity.
- (3) The larger the spray water flow rate of the atomizer, the faster the atomized solution is sprayed out of the atomizer, which did not cause the spray to generate hydrate around the nozzle and block the nozzle. The larger the water jet flow rate, the more hydrate that could be produced continuously, which is an influencing factor to ensure the continuous synthesis of hydrate.

4.3. Influence of the Pressure Difference between the High Pressure Pump and the Reactor on the Synthesis of Hydrate

Due to the existence of air pressure in the reaction kettle, the pressure difference when the pressure pump sprays water into the kettle is lower than the pressure difference when the pressure pump sprays water through the atomizer in the air, which is directly related to the matching selection of the pressure pump and the atomizer. In this experiment, the initial pressure in the reactor was 5 Mpa, the selected atomizer was a conical atomizer, and the pressure gauge of the pressure pump was in the range of 5–5.2 Mpa. While in the air, when the water mist was sprayed by the conical atomizer, the working pressure of the booster pump was between 0–1 Mpa. The spray effect formed by the same atomizer in the air was different from that formed under the experimental pressure of the reactor.

The greater the pressure difference between the high-pressure pump and the reactor, the greater the water flow rate of the atomizer, the smaller the spray angle, and the better the spray atomization effect. Therefore, choosing a pressure pump with a large effective pressure difference under high pressure was more conducive to the formation of hydrate.

4.4. Influence of Experimental Water on Gas Storage Capacity of Synthetic Hydrate

In this experiment, deionized water and ordinary tap water were selected for the experiment. Since the concentration of SDS aqueous solution was in the range of 0.3–1.1 g/L, there was no obvious difference in the synthesis effect of hydrate [16]. Therefore, in the experiment, the concentration of the SDS aqueous solution prepared with deionized water was 0.35 g/L. The concentration of the SDS aqueous solution prepared using tap water was 0.5 g/L. However, under the same conditions, the solution prepared with deionized water was basically clear and transparent after stabilization and the solution prepared with tap water was stabilized with a small amount of flocculent floating. It was speculated that the impurities in the tap water reacted with a small amount of sodium dodecyl sulfate. After the experiment was completed and the drainage was completed, the flocs still existed. The gas storage capacity of natural gas hydrate obtained in the experiment with 0.35 g/L SDS deionized aqueous solution was 1:121, and the gas storage capacity of natural gas hydrate obtained in the experiment with 0.5 g/L SDS tap water solution was 1:123.

Therefore, in the pilot scale, the experimental water had little effect on the gas storage capacity of the generated hydrate.

5. Conclusions

- (1) When the pressure was suitable and constant, temperature was one of the most important factors affecting hydrate formation, decomposition, distribution, and gas storage. The lower the temperature, the harder and denser the hydrate was, the more concentrated the distribution, the higher the gas storage capacity, and the less the decomposition.
- (2) The smaller the aperture of the atomizer, the better the atomization effect, the faster the formation of hydrate, and the greater the gas storage capacity. The greater the flow rate of water spray, the less likely it was to block the atomizer, and the more sustainable the process of generating hydrate. However, the smaller the pore size, the larger the flow rate of water spray that needed to be matched, otherwise the nozzle blockage was very likely to occur, resulting in the termination of the reaction. Further experiments are needed to obtain the proportional relationship between atomizer aperture and water spray flow.
- (3) The greater the difference between the pressure provided by the high-pressure pump and the pressure in the reactor, the greater the water flow rate of the atomizer. The smaller the spray angle, the better the spray atomization effect and the better the quality of the hydrate produced. Therefore, a pressure pump with a large effective pressure difference was more conducive to the formation of hydrate.
- (4) There was no obvious difference between deionized water and tap water for the synthesis of natural gas hydrate. The economical cost of using tap water as raw material was lower, and the process was simpler and easier to operate.
- (5) In this experiment of six working conditions, the best conditions for synthesizing natural gas hydrate were: a pressure of 5 Mpa, a temperature of $-5\text{ }^{\circ}\text{C}$, a high pressure pump reciprocating the plunger pump, model 4D-SY, a maximum working pressure of 63 Mpa, and a flow rate of 22 L/h. After the water spraying, it was left to stand for more than 60 min and the reaction was terminated after the pressure became stable. Then, a large number of hydrates with high purity could be obtained.

Factors such as the optimal volume of the reactor, the spray angle of the atomizer, and the number of atomizers under the pilot-scale conditions have not been considered in this experiment and it is expected that subsequent experiments could be improved.

Author Contributions: Conceptualization, J.Z., and J.T.; methodology, Q.M.; software, Q.L.; validation, C.D. and Q.M.; formal analysis, C.D. and Y.M.; investigation, Q.M.; resources, C.D.; data curation, C.D.; writing—original draft preparation, Y.M.; writing—review and editing, Y.M.; visualization, C.D. and X.W.; supervision, Q.M.; project administration, C.D. and Y.M.; funding acquisition, C.D. and Y.M. All authors have read and agreed to the published version of the manuscript.

Funding: This scientific research project was funded by the Quality and Technical Supervision Bureau of Shandong Province “Research on the Safety Technical Conditions of Synthetic Natural Gas Hydrate Storage and Transportation Containers” (Project No.: 2015KY19) and the Natural Science Foundation of Chongqing Municipality “Research on the Mechanism of Instability of Sandy Slopes Induced by Natural Gas Hydrate Decomposition” (Project No.: cstc2019jcyj-msxmX0815).

Institutional Review Board Statement: The study did not require ethical approval.

Informed Consent Statement: Not applicable.

Data Availability Statement: All data generated or analysed during this study are included in this published article.

Conflicts of Interest: The authors declare no conflict of interest.

References

1. Zhou, H.; Peng, X.; Ye, Y. *Natural Gas Hydrate*; Ocean Publishing House: Beijing, China, 2000.
2. Wu, C.; Sun, C.; Zhao, K.; Yang, J.; Chen, Y. Advances in natural gas storage and transportation technology for hydrates. *Oil Gas Storage Treat.* **2017**, *2*, 29–35.

3. Hu, G.; Ye, Y.; Zhang, J.; Liu, C.; Wang, J. New progress in hydrate storage and transportation technology—Record of the 6th International Hydra Conference. *Mar. Geol. Dyn.* **2008**, *24*, 17–23.
4. Shirota, H.; Aya, I.; Namie, S. Measurement of Methane Hydrate Dissociation for Application to Natural Gas Storage and Transportation. In Proceedings of the Fourth International Conference of Gas Hydrates, Yokohama, Japan, 19–23 May 2002; pp. 972–977.
5. Fan, S. *Natural Gas Hydrate Storage and Transportation Technology*; Chemical Industry Press: Beijing, China, 2005.
6. Chen, G.; Sun, C.; Ma, Q. *Gas Hydrate Science and Technology*; Chemical Industry Press: Beijing, China, 2007; pp. 1–2.
7. Gudmundsson, J.S.; Borrehaug, A. Frozen hydrate for transport of natural gas. In Proceedings of the 2nd International Conference on Gas Hydrate, Toulouse, France, 2–6 June 1996.
8. Katoh, H.; Fukazawa, K. Development of the Silo for Natural Gas Hydrate (NGH) Pellet. In Proceedings of the 6th International Conference on Gas Hydrates (ICGH 2008), Vancouver, BC, Canada, 6–10 July 2008.
9. Katoh, H.; Fukazawa, K. Development of the Silo for Natural Gas Hydrate (NGH) Pellet. In Proceedings of the 7th International Conference on Gas Hydrates (ICGH 2011), Edinburgh, UK, 17–21 July 2011; p. 571.
10. Mimachi, H.; Takeya, S.; Yoneyama, A.; Hyodo, K.; Takeda, T.; Gotoh, Y.; Murayama, T. Natural Gas Storage and Transportation within Gas Hydrate of Smaller Particle: Size Dependence of Self-Preservation Phenomenon of Natural Gas Hydrate. *Chem. Eng. Sci.* **2014**, *118*, 208–213. [[CrossRef](#)]
11. Shirota, H.; Hikida, K.; Nakajima, Y.; Ota, S.; Takaoki, T.; Iwasaki, T.; Ohgaki, K. Use of Hydrate to Natural Gas Transportation Introduction of Research Project. *Recent Adv. Mar. Sci. Technol.* **2002**, 161–167.
12. Eneota, C.; Odutola, T.O.; Ajiyenka, J.A. Maximizing Gas Utilization Using Gas to Hydrates Technology. *Am. J. Eng. Res. (AJER)* **2018**, *7*, 231–239.
13. Katoh, Y.; Uchida, K.; Takahashi, M.; Iwasaki, T.; Engineering, M. Experimental Research on Mixed Hydrate Pellet Production and Dissociation. In Proceedings of the 5th International Conference on Gas Hydrate, Trondheim, Norway, 13–16 June 2005.
14. Watanabe, S.; Takahashi, S.; Mizubayashi, H.; Murata, S.; Murakami, H. A Demonstration Project of NGH Land Transportation System. In Proceedings of the Manuscript for 6th International Conference on Gas Hydrate, Vancouver, BC, Canada, 6–10 July 2008.
15. Makahashi, M.; Kawamura, T.; Yamamoto, Y.; Ohnari, H.; Himuro, S.; Shakutsui, H. Effect of shrinking microbubble on gas hydrate formation. *J. Phys. Chem.* **2003**, *107*, 2171–2173. [[CrossRef](#)]
16. Javanmardi, J.; Nasrifar, K.; Najibi, S.H.; Moshfeghian, M. Economic evaluation of natural gas hydrate as an alternative for natural gas transportation. *Appl. Therm. Eng.* **2005**, *25*, 1708–1723. [[CrossRef](#)]
17. Belandria, V.; Eslamimanesh, A.; Mohammadi, A.H.; Richon, D. Study of gas hydrate formation in the carbon dioxide hydrogen water systems: Compositional analysis of the gas phase. *Ind. Eng. Chem. Res.* **2011**, *50*, 6455–6459. [[CrossRef](#)]
18. Lee, W.; Baek, S.; Kim, J.D.; Lee, J.W. Effects of salt on the crystal growth and adhesion force of clathrate hydrates. *Energy Fuels* **2015**, *29*, 4245–4254. [[CrossRef](#)]
19. Gudmundsson, J.; Andersson, V.; Levik, O.L.; Parlaktuna, M.M. Natural gas hydrates: A new gas transportation form. *J. Pet. Technol.* **1999**, *4*, 66–67.
20. Guo, Y.; Liang, H.; Guan, Y.; He, B. Effect of quaternary salt on the equilibrium conditions of coalbed methane hydrates. *J. Process Eng.* **2017**, *17*, 873–878.
21. Cheng, X.; Shen, Q.; Ma, X.; Li, A.; Zhan, M. Overview of test mining of natural gas hydrates at home and abroad. *Guangdong Chem. Ind.* **2020**, *47*, 23–26.
22. Jiang, L. Experimental Study on Rapid Synthesis Technology of Natural Gas Hydrates. Master's Thesis, Southwest Petroleum University, Chengdu, China, 2018.
23. Lu, Q.; Song, Y.; Li, X. Experimental study on the hydrate generation kinetics of cyclopentane-methane-water system in the foamer. *Chem. Prog.* **2016**, *35*, 3777–3782.
24. Wang, W. Experimental Study on Natural Gas Hydrate Synthesis under SDS System. Master's Thesis, Southwest Petroleum University, Chengdu, China, 2018.
25. Zhang, B.; Wu, Q.; Wang, Y. The mechanism of surfactants on the induction time of gas hydrate formation. *J. Jilin Univ. (Eng. Ed.)* **2007**, *37*, 239–244.
26. Ma, S.; Wu, Y.; Pan, Z.; Kang, J. Promote the research progress of natural gas hydrate generation factors. *Appl. Chem. Ind.* **2017**, *46*, 163–166.
27. Tang, X.; Sun, Z.; Chen, Z.; Liu, X.; Li, J.; Li, C.; Huang, H. Promoting tetrahydrofuran hydrate formation with copper mesh. *Cryog.* **2018**, *4*, 25–29.
28. Ganji, H.; Manteghian, M.; Zadeh, K.S.; Omidkhan, M.; Mofrad, H.R. Effect of different surfactants on methane hydrate formation rate, stability and storage capacity. *Fuel* **2007**, *86*, 434–441. [[CrossRef](#)]
29. Rogers, R.; Yevi, G.Y.; Swalm, M. Hydrate for Storage of Natural Gas. In Proceedings of the 2nd International Conference on Gas Hydrate, Toulouse, France, 2–6 June 1996; pp. 423–429.
30. Xie, Y.; Liu, D.; Fan, Y.; Xie, Y. Experimental study on the gas storage system of spray natural gas hydrate. *J. Shanghai Univ. Technol.* **2006**, *02*, 68–72.
31. Zhou, C.; Hao, W.; Feng, Z. The orifice bubble method shortens the induction period of natural gas hydrate formation. *Nat. Gas Ind.* **2005**, *25*, 27–29.
32. Hu, H.; Liu, D.; Xie, Y.; Yang, Q. Experimental study on fog-enhanced production of natural gas hydrates. *Xinjiang Oil Nat. Gas* **2006**, *2*, 68–72.

33. Yang, Q.; Liu, D.; Xie, Y.; Hu, H.; Xu, X.; Pan, Y. An experimental system for preparing natural gas hydrates by spraying. *Oil Gas Chem. Ind.* **2006**, *35*, 256–259.
34. Liu, D.; Pan, Y.; Zhou, W.; Hu, H.; Xu, X.; Yang, Q. Characteristics of the process of spraying natural gas hydrates. *J. Shanghai Univ. Technol.* **2007**, *29*, 132–136. [[CrossRef](#)]
35. Zhang, L.; Liu, D.; Zhong, D.; Li, G.; Guo, D. Process design of spray synthesis of natural gas hydrates. *Modernization* **2008**, *10*, 64–67.
36. Hu, H.; Liu, D.; Xie, Y.; Yang, Q. Effect of surfactants in the spray reactor on the preparation of natural gas hydrates. *Qilu Petrochem. Ind.* **2006**, *3*, 256–259.
37. Song, X. Experimental Study on the Synthesis of Natural Gas Hydrates Suitable for Ship Transportation. Master's Thesis, Dalian Maritime University, Dalian, China, 2021.
38. Shi, X. Research on High Efficiency Synthesis Technology of Natural Gas Hydrate Reinforced by Spiral Mixing. Master's Thesis, Qingdao University of Science and Technology, Qingdao, China, 2022.
39. Lin, Y.; Liu, L.; Sun, M.; Chen, C.; Zhang, G.; He, Y.; Wang, F. Rapid formation of methane hydrates with compact agglomeration via regulating the hydrophilic groups of nanopromoters. *AIChE J.* **2020**, *66*, e16296. [[CrossRef](#)]
40. Zhong, Y.; Rogers, R.E. Surfactant effects on gas hydrate formation. *Chem. Eng. Sci.* **2000**, *55*, 4175–4187. [[CrossRef](#)]
41. Ye, Y.; Liu, C.; Meng, Q.; Cheng, J. Experimental Device for Determining the Gas Storage Capacity of Natural Gas Hydrates. Patent No. 201010222113.8, 16 February 2011.
42. Xia, N.; Liu, C.; Ye, Y.; Meng, Q.; Lin, X.; He, X. Study on the method of microscopic laser Raman spectroscopy for the determination of natural gas hydrates. *Rock Mine Test* **2011**, *30*, 416–422.
43. Meng, Q.; Liu, C.; Ye, Y.; Chen, Q. Experimental study on gas storage characteristics of methane hydrates in different systems. *World Sci. Technol. Res. Dev.* **2011**, *33*, 25–28.